

Application Value of 64-slice Multidetector Spiral CT Contrast-enhanced Scan in Maxillofacial Soft Tissue Hypervascular Tumours

Wen Xin ZHANG¹, Seyiti PAKEZHATI¹, Shu LIU¹, Xiao Feng HUANG², Guo Wen SUN³, Tie Mei WANG¹

Objective: To evaluate the diagnostic ability and clinical imaging features in maxillofacial soft tissue hypervascular tumours by 64-slice multidetector spiral computed tomography (64-MDCT) contrast-enhanced scanning.

Methods: In a retrospective study of 21 cases of hypervascular tumours, the degree of blood supply and indexes were assessed, and the pathological results were used as the diagnostic gold standard to evaluate the sensitivity and specificity of 64-MDCT plain scan and enhanced CT in the diagnosis of oral and maxillofacial soft tissue hypervascular tumours, using the receiver operating characteristic curve to analyse and evaluate the efficacy.

Results: Among 21 patients, the diagnostic accuracy of 64-MDCT contrast-enhanced scan was 90.48%, the area under the curve of venous phase CT value was 0.80, the sensitivity was 83.30% and the specificity was 72.73%.

Conclusion: 64-MDCT contrast-enhanced scan can be used to evaluate the blood supply of maxillofacial soft tissue hypervascular tumours before an operation. The CT value in the venous phase of tumours has the highest diagnostic effectiveness, which can reduce the risk of blood loss during surgery for maxillofacial hypervascular tumours. In addition, it has certain guiding significance for the formulation of clinical treatment plans.

Key words: contrast-enhanced computed tomography, hypervascular tumours, oral and maxillofacial, radiology, squamous cell carcinoma

Chin J Dent Res 2023;26(2):105–111; doi: 10.3290/j.cjdr.b4128033

More than 650,000 cases of maxillofacial and neck tumours are diagnosed worldwide every year, with a higher rate in Asia¹. Maxillofacial soft tissue hypervascular tumours are tumors with special physiological characteristics affecting the head and neck, which increases the risk and difficulty of operation due to the complex anatomical structure and abundant blood supply, and they also involve multiple anatomical areas

including the oral cavity, pharynx, larynx, paranasal sinuses, nasal cavity and salivary glands.

Previous studies have focused mainly on benign hypervascular tumours such as hemangioma and vascular malformation^{2,3}, but few have studied other soft tissue hypervascular tumours in the maxillofacial region. The physiological characteristics of malignant tumours such as oral squamous cell carcinoma (OSCC) and other benign tumours can match those of hypervascular tumours⁴.

It is particularly important to evaluate the blood supply of a tumour accurately before an operation, choose the appropriate surgical path and reduce the chances of injury in patients. In addition, implementation of multidimensional visualisation of tumours can objectively and truly show the relationship between tumours, blood vessels, jaws, the degree of blood supply of the tumour and the normal anatomy and pathological changes of blood supplying arteries and surrounding blood vessels, providing more accurate auxiliary diag-

1 Department of Dentomaxillofacial Radiology, Nanjing Stomatological Hospital, Medical School of Nanjing University, Nanjing, P.R. China.

2 Department of Oral Pathology, Nanjing Stomatological Hospital, Medical School of Nanjing University, Nanjing, P.R. China.

3 Department of Oral and Maxillofacial Surgery, Nanjing Stomatological Hospital, Medical School of Nanjing University, Nanjing, P.R. China.

Corresponding author: Dr Tie Mei WANG, Department of Dentomaxillofacial Radiology, Nanjing Stomatological Hospital, Medical School of Nanjing University, Zhong Yang Road 30, Nanjing 210008, P.R. China. Tel: 86-25-83620351; Fax: 86-25-83620200. Email: tiemeiwang106@163.com

nosis and treatment plans for stomatologists, which is also a pressing clinical issue to solve and address.

Studies have shown that computed tomography (CT) image features correlate with the histopathological grade, molecular biomarkers and prognosis for various tumours, such as oropharyngeal, oesophageal and breast cancer⁵. Using contrast-enhanced imaging, Yu et al⁶ distinguished between human papillomavirus positive and negative oropharyngeal cancers.

In the present study, we analysed CT-based radiological features of maxillofacial soft tissue hypervascular tumours based on the ability of these features to predict important clinical and histological factors across different tumour types.

Materials and methods

Case selection

This retrospective study was conducted in accordance with the Declaration of Helsinki (as revised in 2013) and approved by the institutional review board of Nanjing University Medical College Affiliated Stomatology Hospital (NJSH-2022NL-011). The case records were identified in our institution from June 2017 to October 2021. A total of 21 patients with a diagnosis of maxillofacial soft tissue hypervascular tumours (15 men and 6 women; mean age 47.57 ± 16.45 years) were enrolled in this study. The inclusion criteria were as follows:

- patients with plain CT scan and multidetector spiral CT (64-MDCT) enhanced examination prior to surgery;
- arterial phase net enhancement value exceeding flat scan CT value ≥ 40 Hu after enhancement of the CT scan, which could be diagnosed using imaging.

The exclusion criteria were as follows:

- patients with hyperthyroidism, asthma, liver, kidney or severe cardiopulmonary insufficiency, or who are not well and may be in danger during the image-taking process;
- patients with iodine contrast agent allergy, history of drug allergy and allergic constitution;
- female patients who were planning pregnancy within 6 months or who were pregnant or lactating;
- patients who were unable to cooperate;
- images including metal ornaments and foreign objects, as well as obvious motion artefacts.

Criteria for judging enhancement

If the lesion had vascular imaging or the difference between CT images before and after enhancement exceeded 40 Hu, it was defined as “enhanced”; if it did not have a vascular shadow or the difference between CT images before and after enhancement was between 20~40 Hu, it was defined as “possible enhancement”; and if no vascular shadow was seen or the difference between CT images before and after enhancement was less than 20 Hu, it was considered “no enhancement”⁷.

CT image acquisition

CT examinations were performed on a 64-slice CT scanner (SOMATOM Perspective Sensation 64, Siemens Healthineers, Erlangen, Germany). A CT scan of the head and neck was performed, followed by contrast-enhanced 64-MDCT examination. The scanning range was from the aortic arches to the cranial top. Scan parameters were set at 110 kV, and the pipe current was automatically adjusted by the CT machine based on the CARE Dose4D (Siemens) intelligent algorithm, 64×0.625 mm detector collimation, gantry rotation time of 0.48 seconds and slice thickness of 1 mm. CT scans of the head and neck were performed using intravenous nonionic iodinated contrast (350 mg/ml, Iohexol). The dosage of contrast agent was calculated according to patients' weight as 1.5 to 2.0 ml/kg to inject at 3.5 ml/second. The follow-up scan was delayed by 10 seconds after the start of contrast injection. The tracking scan interval was 1 seconds. When the CT value of the aortic arch area reached 95 Hu, the arterial period scan was begun.

Image analysis

CT feature evaluation

Two radiologists with 8 and 12 years of experience and who were blinded to the pathological diagnosis performed CT analysis independently. The following CT features were evaluated qualitatively:

- lesion size (expressed as the largest dimension);
- tumour margin (clear or unclear);
- area of the tumour;
- necrosis (absent or present);
- texture (uniform or non-uniform);
- CT value and CT enhancement value of each phase (the diameter of the region of interest [ROI] set at 1 cm.

Table 1 Clinical data and CT signs of benign and malignant tumors with a rich blood supply in the oral and maxillofacial region.

Clinical factors and image feature		Malignant [cases (%)]	Benign [cases (%)]	P value
Sex (M/F)		10/2	5/4	0.16
Age (y)		50.67 ± 13.11 (33 ~67)	43.44 ± 20.17 (17~68)	0.03
Location	Oropharynx	4 (33.3)	2 (22.2)	0.46
	Tongue	2 (16.7)	NA (NA)	
	Neck	1 (8.3)	NA (NA)	
	Parotid	2 (16.7)	3 (33.3)	
	Buccal	3 (25.0)	4 (44.4)	
Margin (clear or unclear)		8/4	8/1	0.16
Necrosis (absent or present)		4/8	2/7	0.58
Texture (uniform or non-uniform)		4/8	3/6	1.00
CT value (Hu)	Plain CT	49.08 ± 8.77	46.85 ± 7.10	0.84
	Arterial phases	104.71 ± 27.37	152.09 ± 63.63	0.01
	Venous phases	103.92 ± 16.09	143.32 ± 67.04	0.03
	Arterial phase net enhancement value	55.63 ± 28.24	105.00 ± 65.03	0.01
	Venous phase net enhancement value	54.84 ± 16.52	96.37 ± 66.62	0.01

F, female; M, male; NA, not applicable.

Table 2 Comparison of plain scan and contrast-enhanced 64-MDCT in the area of maxillofacial soft tissue hypervascular tumours.

Group	Area (mm ²)	P value
Plain CT scan	10.84 ± 7.13	0.00
Contrast-enhanced 64-MDCT	12.13 ± 7.03	

The most obvious tumour enhancement area was selected to avoid the volume effect and artefact area, and the mean value was measured.

Enhanced performance

Based on the combination of contrast enhancement observed at each stage of the study, a global dynamic pattern of enhancement was defined. Stable contrast enhancement referred to stable and persistent enhancement in which all or part of the lesions in the arterial phase are higher than the surrounding soft tissue, and progressive contrast enhancement was where the lesion increases progressively over time, reaching maximal intensity in venous phases; these classifications were adopted from Iavarone et al⁸.

Statistical analysis

Statistical analysis was performed using SPSS (IBM, Armonk, NY, USA). Chi-square or Fisher exact tests and independent sample *t* tests were used for qualitative and quantitative data, respectively. Associated receiver operating characteristic (ROC) curves were plotted using SPSS. Intragroup correlation coefficient (ICC) was used to evaluate the consistency of CT values measured

by two doctors. *P* < 0.05 was considered statistically significant.

Results

The CT data measured by two radiologists were demonstrated to have a good agreement, with ICCs of 0.92. The characteristics of the patients are described in Table 1. There were significant differences in patient age between the two groups (*P* < 0.05). Patients with malignant hypervascular tumours were older than their counterparts with benign tumours. The lesion area showed significant differences between the group with plain CT scans and contrast-enhanced CT scans (*P* < 0.00), showing that the tumour boundary after enhancement is larger than that for the plain CT scan image. Comparisons of the two groups are presented in Table 2.

Contrast-enhanced CT provided the best accuracy in detecting benign and malignant maxillofacial soft tissue hypervascular tumours (90.48%), and it was superior to plain scans (14.29%). The exact values are shown in Table 3.

With a threshold of 0.73, the sensitivity of the venous phase CT value and the venous phase net enhancement value was 83.30% and 100.00%, respectively, and the specificity was 72.73%. The area under the curve (AUC)



Table 3 Comparison of the diagnostic accuracy of plain scan and contrast-enhanced 64-MDCT in maxillofacial hypervascular tumours.

Group	Diagnosis result		Diagnosis rate (%)
	+	-	
Plain CT scan	3	18	14.29
Contrast-enhanced 64-MDCT	19	2	90.48
χ^2	24.44		
P value	0.00		

Table 4 ROC curve results of different CT value indexes to evaluate the degree of blood supply of maxillofacial soft tissue hypervascular tumours.

Variable	AUC	P value	SE	95% CI	Sensitivity (%)	Specificity (%)	Youden index
Arterial phase	0.74	0.06	0.12	0.51–0.90	95.20	54.55	0.55
Arterial phase net enhancement value	0.73	0.07	0.12	0.50–0.89	100.00	54.55	0.55
Venous phase	0.80	0.01	0.12	0.59–0.94	83.30	72.73	0.73
Venous phase net enhancement value	0.76	0.05	0.13	0.54–0.91	100.00	72.73	0.73

CI, confidence interval; SE, standard error.

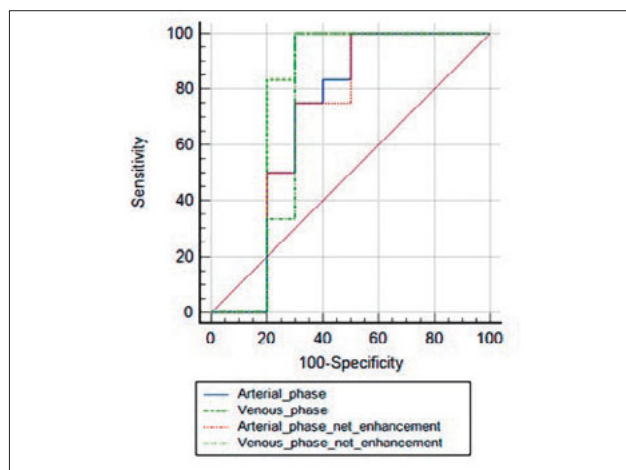


Fig 1 The ROC curve of contrast-enhanced 64-MDCT to evaluate the blood supply to a maxillofacial soft tissue hypervascular tumour.

for ROC analysis was 0.80 and 0.76. Sensitivity and specificity are presented in Table 4 and Fig 1.

Discussion

Hypervascular tumours

A soft tissue hypervascular tumour is a type of tumour or tumour-like lesion with a net enhancement degree of arterial and venous phase equal to or greater than that of a plain CT scan, as well as increased intensity after enhanced CT⁹. Blood-rich tumours of the head and neck include hemangioendothelioma, neurogenic tumours

(e.g., schwannoma), paragangliomas (e.g., carotid body tumours), nasopharyngeal angiofibromas, hemangiomas and other malignant tumours¹⁰. The present study involved nine cases of soft tissue benign tumours, including spindle cell tumor (one case), basal cell adenoma (one case), adenolymphoma (one case) and inflammatory mass (one case). There were five cases of vasogenic tumours, including vascular malformation (four cases) and carotid body tumour (one case). Twelve cases of malignant blood-rich tumours included squamous cell carcinoma (nine cases), mucoepidermoid carcinoma (one case), acinar cell carcinoma (one case) and malignant lymphadenoma (one case). In the diagnosis of hypervascular diseases such as affecting the liver and kidney, enhanced 64-MDCT plays an important role in the preoperative examination, showing uniform or inhomogeneous and marginal enhancement in each stage of enhancement and showing “cow’s eye” and “pupil” sign (the centre of the lesion is low density, the edge is high density due to enhancement, and the density of the outermost layer of the lesion is lower than that of normal tissue) when the lesion is necrotic¹¹.

With regard to tumours with a rich blood supply in the maxillofacial soft tissue, on the plain CT scan, most soft tissue masses had a uniform density and unclear boundary and showed round, quasi-round or irregular soft tissue mass after enhancement. In this study, most of the benign tumours were vascular lesions (5 seconds, 9%). The boundary was clear after enhancement and the lesions were significantly enhanced in uniform mass and patch shape. The interior and edges were characterised by clusters of enhanced blood ves-

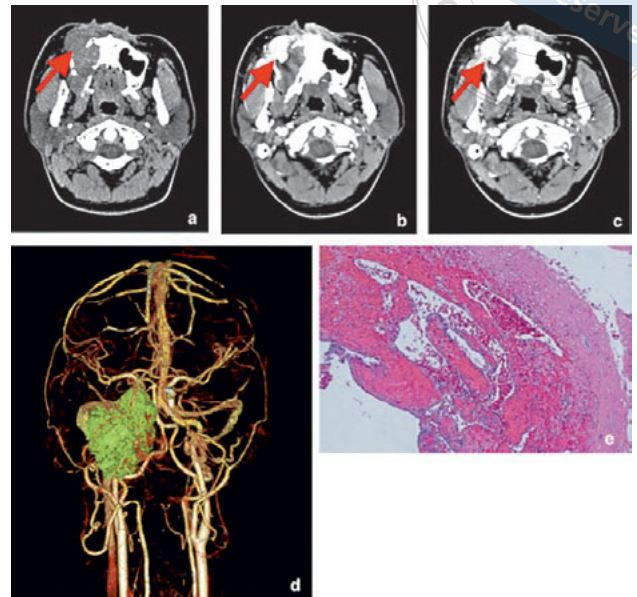


Fig 2 A 24-year-old man with vascular malformation of the right maxilla. (a) The plain scan image shows the soft tissue mass in the right maxilla, the CT value is around 56 Hu, and the boundary is not clear. (b) The CT value of the arterial phase is 178 Hu. (c) The CT value of the venous phase is 236 Hu, showing rosette-shaped and patch-like enhancement. (d) Volume rendering technique reconstruction images show that the boundary of the mass is adjacent to the internal carotid artery and there are branches of the external carotid artery passing through it. (e) Inflammatory fibrous connective tissue and bone tissue, with vascular hyperplasia and a large number of cellulose hemorrhagic exudation. (hematoxylin-eosin, original magnification $\times 100$).

sels and vascular penetration of varying thickness. On the other hand, benign tumours of the parotid gland, such as basal cell adenoma, show severe enhancement in the venous phase, which is generally weakened further in the delayed phase, and cystic changes are easy to observe. This may be related to the vascular structure of the tumour; the cystic area contains many endothelial-lined vascular channels, as well as capillaries and venules¹². The enhancement of inflammatory components in this group of tumours shows solid tissue with an irregular shape. Pathology suggests that chronic inflammation with necrosis may be caused by infection, and a large amount of neovascularisation is formed during the repair process of inflammation and necrosis¹³. The majority of malignant or metastatic tumours showed inhomogeneous rosette-like and patchy severe enhancement, which was further enhanced in the venous phase; additionally, these tumours were different to malignant hypervascular tumours of the liver, which often show “fast-in and fast-exit” patterns. The solid components of malignant hypervascular tumours in the maxillofacial region were significantly enhanced and mixed with uneven enhancement areas, which represented the vascular nutrient area, tumour cell aggregation area and necrotic area within the tumour. In addition, delayed enhancement is related to the content and composition of collagen fibres in the tumour¹⁴.

According to the results of the ROC curve analysis, enhanced 64-MDCT is a more effective and sensitive method for screening and predicting hypervascular tumours in the maxillofacial region because it gives the

largest AUC of venous phase CT scans, which is useful in determining the degree and characteristics of the tumour’s blood supply. The present results indicate that when the enhanced CT value of the tumour is ≥ 80 Hu, it can be considered to have a rich blood supply. The results also suggest that when the tumour displays progressive enhancement and the venous phase CT value reaches 112~131 Hu, it can be regarded as a malignant hypervascular tumour.

In this study, the diagnostic accuracy of enhanced 64-MDCT is much higher than that of a plain scan with enhanced CT, indicating that contrast-enhanced CT can dynamically distinguish between blood vessels and lymph nodes, clearly display the location, size, boundary, blood supply and surrounding tissue infiltration of the mass, and provide more vascular anatomical information and a stereoscopic view combined with image post-processing¹⁵.

The present authors found that the size of the lesion measured by the plain scan of a maxillofacial soft tissue tumour with a rich blood supply was smaller than its numerical boundary measured after enhancement and that this was likely due to marginal infiltration of the tumour, which included increased neovascularisation and blood flow at the margins. The surface permeability is high, which increases expression in the marginal tissue of the tumour¹⁶. The case is shown in Figs 2 and 3.

Treatment

Surgery and/or intervention forms the basis for the treatment of soft tissue hypervascular tumours¹⁷, and

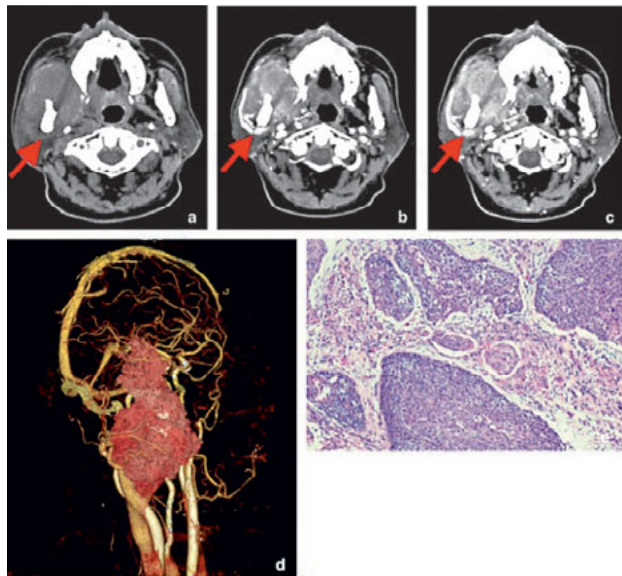


Fig 3 A 67-year-old man with squamous cell carcinoma of the maxillary right posterior area. **(a)** The plain scan image shows the soft tissue mass in the maxillary right posterior area. The CT value is around 42 Hu. **(b)** The CT value of the arterial phase is 97 Hu. **(c)** The CT value of the venous phase is 114 Hu and the boundary is clear, showing target-like enhancement. **(d)** Volume rendering technique reconstruction images show that the mass is adjacent to the external carotid artery. **(e)** There was obvious epithelial nest mass infiltration with necrosis in the maxillary right posterior area (hematoxylin-eosin, original magnification $\times 100$).

requires accurate information about the location, size and extent of the lesions, as well as blood supply and drainage vessels. Thus, the analysis and prediction of preoperative noninvasive imaging examination are very important for treatment planning. Enhanced 64-MDCT can predict the degree of the tumour blood supply in relation to the rich blood supply to the soft tissue, as well as the relationship between the tumour, blood vessel and maxillofacial bone¹⁸, which is used by clinicians to design operating plans and assess operational risks. The radiation dose and iodine contrast agent used in enhanced 64-MDCT are lower than in catheter angiography. Additionally, it has the advantages of no anaesthesia intubation, no obvious trauma¹⁹ and higher sensitivity and visibility than ultrasound and other noninvasive imaging²⁰.

Application value

64-MDCT contrast-enhanced technology also has high application value for tumours adjacent to or invading the internal carotid artery. Contrast-enhanced CT can show the relationship between tumours and carotid artery through 64-MDCT contrast-enhanced technology, clarify the situation of wrapping, passing, erosion and the intracranial circle of Willis, and provide a basis for surgical plan design. If the internal carotid artery is only moved but not eroded, the internal carotid artery can be preserved. If the internal carotid artery is extensively eroded, the preoperative plan should be designed carefully to make preparations and plans in advance for the sacrifice of the internal carotid artery, which can avoid the serious con-

sequences of intracranial ischemia caused by temporary ligation or sacrifice of the internal carotid artery during the operation. Some cervical hemangiomas located in the skull base, penetrating through the skull or rich in blood supply, including carotid body tumours, nasopharyngeal hemangioma and mild hemangiopericytoma, are difficult to operate, which can be done with 64-MDCT contrast-enhanced scans aided by preoperative embolisation therapy to reduce intraoperative bleeding and increase the success rate of surgery for patients. For large-scale aneurysmal bone cysts, cementum-ossifying fibroma, malignant tumours of the inferior temporal fossa and metastatic tumours, preoperative 64-MDCT contrast-enhanced scan evaluation can also be performed. If the risk of intraoperative bleeding is high and the lesion cannot be completely resected, preoperative embolisation can be performed.

Conclusion

In this study, 64-slice spiral CT plain scan and contrast-enhanced CT were used to evaluate the blood supply of oral and maxillofacial soft tissue tumours. The results showed high sensitivity and good repeatability of the noninvasive imaging evaluation. The present study provides the theoretical basis and a certain clinical significance and reference value for preventing tumour recurrences. In addition, we also used 3D reconstruction technology to more intuitively and clearly show the relationship between tumour and surrounding blood vessels, bone and other anatomical structures to provide guidance for clinical analysis.

Conflicts of interest

The authors declare no conflicts of interest related to this study.

Author contribution

Drs Wen Xin ZHANG, Seyiti PAKEZHATI and Shu LIU collected data and draft the manuscript; Drs Xiao Feng HUANG and Guo Wen SUN provided clinical data and pictures; Dr Tie Mei WANG proposed revisions during the review of this paper. All authors agreed with the final version of the manuscript.

(Received Oct 31, 2022; accepted Feb 20, 2023)

References

1. Shang C, Feng L, Gu Y, Hong H, Hong L, Hou J. Impact of multi-disciplinary team management on the survival rate of head and neck cancer patients: A cohort study meta-analysis. *Front Oncol* 2021;11:630906.
2. Choi JH, Ro JY. The 2020 WHO classification of tumors of bone: An updated review. *Adv Anat Pathol* 2021;28:119–138.
3. Gong QX, Fan QH. Updates of the 2020 WHO classification of soft tissue tumors: part II [in Chinese]. *Zhonghua Bing Li Xue Za Zhi* 2021;50:314–318.
4. Agarwal D, Pardhe N, Bajpai M, et al. Characterization, localization and patterning of lymphatics and blood vessels in oral squamous cell carcinoma: A comparative study using D2-40 and CD-34 IHC marker. *J Clin Diagn Res* 2014;8:ZC86–ZC89.
5. Zhang MH, Hasse A, Carroll T, Pearson AT, Cipriani NA, Ginat DT. Differentiating low and high grade mucoepidermoid carcinoma of the salivary glands using CT radiomics. *Gland Surg* 2021;10:1646–1654.
6. Yu K, Zhang Y, Yu Y, et al. Radiomic analysis in prediction of human papilloma virus status. *Clin Transl Radiat Oncol* 2017;7:49–54.
7. Hartman DS, Choyke PL, Hartman MS. From the RSNA refresher courses: A practical approach to the cystic renal mass. *RadioGraphics* 2004; 24(suppl 1):S101–S115.
8. Iavarone M, Piscaglia F, Vavassori S, et al. Contrast enhanced CT-scan to diagnose intrahepatic cholangiocarcinoma in patients with cirrhosis. *J Hepatol* 2013;58:1188–1193.
9. Choi HH, Manning MA, Mehrotra AK, Wagner S, Jha RC. Primary hepatic neoplasms of vascular origin: Key imaging features and differential diagnoses with radiology-pathology correlation. *AJR Am J Roentgenol* 2017;209:W350–W359.
10. Lutz J, Holtmannspötter M, Flatz W, et al. Preoperative embolization to improve the surgical management and outcome of juvenile nasopharyngeal angiofibroma (JNA) in a single center: 10-year experience. *Clin Neuroradiol* 2016;26:405–413.
11. Wang G, Zhu S, Li X. Comparison of values of CT and MRI imaging in the diagnosis of hepatocellular carcinoma and analysis of prognostic factors. *Oncol Lett* 2019;17:1184–1188.
12. Chen G, Wen X, Chen XJ, et al. Imaging features and pathological analysis of 43 parotid basal cell adenomas. *Comput Math Methods Med* 2021;2021:7906058.
13. Wang H, Li QK, Auster M, Gong G. PET and CT features differentiating infectious/inflammatory from malignant mediastinal lymphadenopathy: A correlated study with endobronchial ultrasound-guided transbronchial needle aspiration. *Radiol Infect Dis* 2018;5:7–13.
14. Papatnassiou ZG, Alberghini M, Picci P, et al. Solitary fibrous tumors of the soft tissues: Imaging features with histopathologic correlations. *Clin Sarcoma Res* 2013;3:1.
15. Ren Y, Chen GZ, Liu Z, Cai Y, Lu GM, Li ZY. Reproducibility of image-based computational models of intracranial aneurysm: A comparison between 3D rotational angiography, CT angiography and MR angiography. *Biomed Eng Online* 2016;15:50.
16. Wong C, Stylianopoulos T, Cui J, et al. Multistage nanoparticle delivery system for deep penetration into tumor tissue. *Proc Natl Acad Sci U S A* 2011;108:2426–2431.
17. Su LX, Fan XD, Zheng JW, et al. A practical guide for diagnosis and treatment of arteriovenous malformations in the oral and maxillofacial region. *Chin J Dent Res* 2014;17:85–89.
18. Corriere MA, Islam A, Craven TE, Conlee TD, Hurie JB, Edwards MS. Influence of computed tomography angiography reconstruction software on anatomic measurements and endograft component selection for endovascular abdominal aortic aneurysm repair. *J Vasc Surg* 2014;59:1224–1231.e1–e3.
19. Zhao Y, Yang L, Wang Y, Zhang H, Cui T, Fu P. The diagnostic value of multi-detector CT angiography for catheter-related central venous stenosis in hemodialysis patients. *Phlebology* 2021;36:217–225.
20. Swieton D, Kaszubowski M, Szyndler A, et al. Visualizing carotid bodies with Doppler ultrasound versus CT angiography: Preliminary study. *AJR Am J Roentgenol* 2017;209:1348–1352.